 CMES, vol.29, no.2, pp.63-73, 2008

A Boundary Element Formulation for Boundary Only Analysis of Thin Shallow Shells

E. L. Albuquerque[1] and M. H. Aliabadi[2]

Abstract: This paper presents a boundary element formulation for the analysis of thin shallow shells. Classical plate bending and plane elasticity formulations are coupled and effects of curvature are treated as body forces. The body forces are written as a sum of approximation functions multiplied by coefficients. Domain integrals that arise in the formulation are transformed into boundary integrals by the radial integration method. Two different approximation functions are employed, that is $1+r$ and $r^2 \log r$. The method is applied to several problems and the accuracy of each approximation function is assessed by comparison with results from literature.

Keyword: Boundary element method, radial integration method, shallow shells

1 Introduction

Shallow shells have been analysed by different numerical methods, for example, finite element method [Brebbia and Debnath (1970)], boundary element method [Lu and Huang (1992), Dirgantara and Aliabadi (1999)], and meshless method [Li, Soric, Jarak, and Atluri (2005) and Rabckzuk and Areias (2006)]. Considerable progress has been made in the past few years in application of the boundary element method (BEM) to the analysis of shell structures. One of the first works was due to Newton and Tottenham (1968) who presented an application of the BEM to shallow shells by decomposition of the fourth order governing equation into a second order equation. Since this work, many different approaches have been developed [see review by Beskos (1991)]. In some formulations there is no domain integration, as Lu and Huang (1992) who developed a direct BEM for shallow shells involving shear deformation. However, the direct BEM involves complicated fundamental solutions. An alternative to the direct BEM is the coupling of plate bending and plane elasticity formulations, as proposed by Zhang and Atluri (1986) who derived a formulation for static and dynamic analysis of classical shallow shells. The domain integrals were computed by domain discretization into cells. This formulation was extend for nonlinear problems by Zhang and Atluri (1986,1988). Later, Dirgantara and Aliabadi (1999) presented a formulation to the analysis of shear deformable shallow shells. However, the discretization of the domain into cells reduces one of the main advantages of the BEM that is the boundary only discretization. Later, Wen, Aliabadi, and Young (2000) used the formulation proposed by Dirgantara and Aliabadi (1999) and transformed the domain integrals into boundary integrals using the dual reciprocity method. Baiz and Aliabadi (2006) presented a boundary element formulation for the analysis of linear buckling of shear deformable shallow shells.

The dual reciprocity method (DRM) and the radial integration method (RIM) are two techniques used in the BEM to transform domain integrals into boundary integrals. Details of the DRM can be found for example in Partridge, Brebbia, and Wrobel (1992) and of the RIM in Gao (2002) and in Albuquerque, Sollero, and Paiva (2007). These methods are suitable for boundary element formulations where a complete fundamental solution is either unavailable or very complex, because in these cases one or more terms can remain as domain integrals in order to use a simpler fundamen-

[1] Faculty of Mechanical Engineering, State University of Campinas, 13083-970, Campinas, Brazil, Currently at Imperial College London, UK, as an Academic Visitor

[2] Department of Aeronautics, Imperial College London, London, SW7 2AZ, UK

tal solution. Thus, a large number of problems can be solved with the knowledge of few fundamental solutions and additional terms, as inertia or nonlinear effects, can be treated as body forces and taken to the boundary. In both methods, the remaining terms are approximated through a finite series expansion involving proposed approximating functions and coefficients to be determined. This expansion is substituted in the generated domain integrals that are, subsequently, transformed into boundary integrals. The main difference between DRM and RIM is that in the second there is no need to compute particular solutions. In addition, using DRM to shell problems would require the evaluation of transversal displacement by derivatives of the radial bases approximation function [see Wen and Aliabadi (2000)]. To the best of authors knowledge, it hasn't been found in literature any work where the RIM has been applied to shell formulations. The boundary element formulation for shells using RIM has not been reported previously.

In this paper, a boundary element formulation for thin shallow shells with no domain discretization is presented. The domain integrals due to the curvature of the shells are transformed into boundary integrals using the RIM. Two approximation functions are used. Differences between DRM and RIM are discussed. Displacements computed using both approximation functions are in good agreement with results available in literature.

2 Boundary integral equations

Consider a shallow shell of an isotropic elastic material with the mid-surface being described by $z = z(x_1, x_2)$ as shown in Figure 1. The base-plane of the shell is defined by a domain Ω in the plane x_1, x_2 whose boundary is given by Γ.

Using equilibrium equations of isotropic shallow shells, the reciprocity relation, and the Green theorem, Zhang and Atluri (1986) derived integral equations that can be divided in terms of plane elasticity and plate bending formulations. These formulations are coupled by the domain integrals that arise in equations. Plane elasticity integral

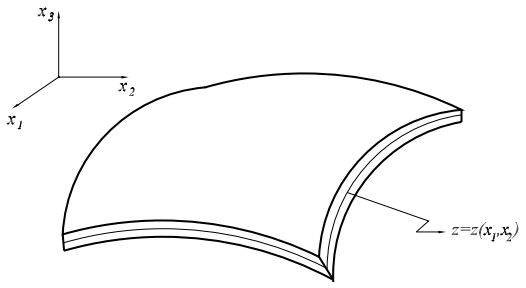

Figure 1: Shallow shell.

equations (membrane equations) are given by:

$$
\begin{aligned}
& c_{ij}u_j + \int_\Gamma t^*_{ik}(Q,P)u_k(P)d\Gamma(P) \\
& = \int_\Gamma u^*_{ik}(Q,P)t_k(P)d\Gamma(P) \\
& + \int_\Omega C\kappa_{kj}wu^*_{ik,j}(Q,P)d\Omega \\
& + \int_\Omega u^*_{ik}(Q,P)q_k(P)d\Omega(P),
\end{aligned} \tag{1}
$$

where $i, j, k = 1, 2$; u_k is the displacement in directions x_1 and x_2, $t_i = N_{ij}n_j$, N_{ij} are membrane forces applied in the shell; w stands for the displacement in the normal direction of the shell surface; q_k are domain loads applied in directions of axis x_1 and x_2; P is the field point; Q is the source point. The constant c_{ij} is introduced in order to take into account the possibility that the point Q can be placed in the domain, on the boundary, or outside the domain. The symbol * stands for fundamental solutions (see Aliabadi, 2002). Constant κ_{kj} depends on the curvature radii R_{kj} of the shallow shell and are given by:

$$
\begin{aligned}
\kappa_{11} &= \frac{1}{R_{11}} + \frac{\nu}{R_{22}} \\
\kappa_{22} &= \frac{\nu}{R_{11}} + \frac{1}{R_{22}} \\
\kappa_{12} &= \frac{1-\nu}{R_{12}}
\end{aligned} \tag{2}
$$

The plate bending integral equation is given by:

$$
\begin{aligned}
& Kw(Q) \\
& + \int_\Gamma \left[V^*_n(Q,P)w(P) - m^*_n(Q,P)\frac{\partial w(P)}{\partial n} \right] d\Gamma(P)
\end{aligned}
$$

$$
\begin{aligned}
&+\sum_{i=1}^{N_c} R^*_{c_i}(Q,P)w_{ci}(P) = \sum_{i=1}^{N_c} R^*_{c_i}(P)w_{ci}(Q,P)\\
&+\int_\Omega q_3(P)w^*(Q,P)\,d\Omega\\
&+\int_\Gamma \left[V_n(P)w^*(Q,P) - m_n(P)\frac{\partial w^*}{\partial n}(Q,P)\right] d\Gamma(P)\\
&+\int_\Gamma C\kappa_{ij}n_j u_i(P)w^*(Q,P)\,d\Gamma(P)\\
&+\int_\Omega C\frac{\kappa_{ij}}{\rho_{ij}}w^*(Q,P)w(P)\,d\Omega\\
&+\int_\Omega \left[C\kappa_{ij}(P)w^*(Q,P)\right]_{,j} u_i(P)\,d\Omega, \qquad (3)
\end{aligned}
$$

where $\frac{\partial()}{\partial n}$ is the derivative in the direction of the outward vector $\mathbf{n}$ that is normal to the boundary Γ; m_n and V_n are, respectively, the normal bending moment and the Kirchhoff equivalent shear force on the boundary Γ; R_c is the thin-plate reaction of corners; w_{ci} is the transverse displacement of corners; q_3 is the domain force in the transversal direction; K is a constant equivalent to c_{ij} of equation (1).

In order to have an equal number of equations and unknowns, it is necessary to write an integral equation corresponding to the derivative of the displacement $w(Q)$ in relation to the unity vector $\mathbf{m}$ that is normal to the boundary in the source point Q. This equation is given by:

$$
\begin{aligned}
&K\frac{\partial w}{\partial m}(Q)\\
&+\int_\Gamma \left[\frac{\partial V^*_n(Q,P)}{\partial m}w(P) - \frac{\partial m^*_n(Q,P)}{\partial m}\frac{\partial w(P)}{\partial n}\right]\\
&d\Gamma(P) + \sum_{i=1}^{N_c}\frac{\partial R^*_{c_i}(Q,P)}{\partial m}w_{ci}(P)\\
&= \sum_{i=1}^{N_c}\frac{\partial R_{c_i}(P)^*}{\partial m}w_{ci}(Q,P)\\
&+\int_\Omega q_3(P)\frac{\partial w^*(Q,P)}{\partial m}d\Omega\\
&+\int_\Gamma \left[V_n(P)\frac{\partial w^*(Q,P)}{\partial m} - m_n(P)\frac{\partial^2 w^*}{\partial n\partial m}(Q,P)\right]\\
&d\Gamma(P) + \int_\Gamma C\kappa_{ij}n_j u_i(P)\frac{\partial w^*(Q,P)}{\partial m}d\Gamma(P)\\
&+\int_\Omega C\frac{\kappa_{ij}}{\rho_{ij}}\frac{\partial w^*(Q,P)}{\partial m}w(P)\,d\Omega\\
&+\int_\Omega \left[C\kappa_{ij}(P)\frac{\partial w^*(Q,P)}{\partial m}\right]_{,j} u_i(P)\,d\Omega. \qquad (4)
\end{aligned}
$$

As can be seen in equations (1), (3), and (4), domain integrals arise in the formulation owing to the curvature of the shell. These domain integrals are:

$$P_1(Q) = \int_\Omega C\kappa_{kj}wu^*_{ik,j}(Q,P)d\Omega, \qquad (5)$$

$$P_2(Q) = \int_\Omega C\frac{\kappa_{ij}}{\rho_{ij}}w^*(Q,P)w(P)\,d\Omega, \qquad (6)$$

$$P_3(Q) = \int_\Omega \left[C\kappa_{ij}(P)w^*(Q,P)\right]_{,j} u_i(P)\,d\Omega, \qquad (7)$$

$$P_4(Q) = \int_\Omega C\frac{\kappa_{ij}}{\rho_{ij}}\frac{\partial w^*(Q,P)}{\partial m}w(P)\,d\Omega, \qquad (8)$$

and

$$P_5(Q) = \int_\Omega \left[C\kappa_{ij}(P)\frac{\partial w^*(Q,P)}{\partial m}\right]_{,j} u_i(P)\,d\Omega. \qquad (9)$$

In order to transform these integrals into boundary integrals, the RIM is used. Details of this method can be found in Albuquerque, Sollero, and Paiva (2007). However, for sake of completeness, some steps of the method are repeated here, in the next section.

3 The radial integration method

Consider, in a general case, the following domain integration:

$$P(Q) = \int_\Omega b(P)v^*(Q,P)d\Omega, \qquad (10)$$

where b and v^* are generic body force and fundamental solution, respectively.

The body force is approximated over the domain Ω as a sum of M products between approximation functions f_m and unknown coefficients γ_m, that is:

$$b(P) = \sum_{m=1}^{M}\gamma_m f_m \qquad (11)$$

for approximation functions based on pure radial basis function, or

$$b(P) = \sum_{m=1}^{M}\gamma_m f_m + ax + by + c \qquad (12)$$

with

$$\sum_{m=1}^{M} \gamma_m x_m = \sum_{m=1}^{M} \gamma_m y_m = \sum_{m=1}^{M} \gamma_m = 0 \tag{13}$$

for approximation functions based on radial basis function combined with augmentation functions.

Now, considering that the body force is approximated, for simplicity, by equation (11), the domain integral (10) can be written as:

$$\begin{aligned} P(Q) &= \int_{\Omega} b(P) v^*(Q,P) d\Omega \\ &= \sum_{m=1}^{M} \gamma_m \int_{\Omega} f_m v^*(Q,P) d\Omega, \end{aligned} \tag{14}$$

or

$$P(Q) = \sum_{m=1}^{M} \gamma_m \int_{\Omega} f_m v^*(Q,P) \rho d\rho d\theta, \tag{15}$$

or

$$P(Q) = \sum_{m=1}^{M} \gamma_m \int_{\theta} \int_{0}^{r} f_m v^*(Q,P) \rho d\rho d\theta, \tag{16}$$

where r is the value of ρ in a point of the boundary Γ.

Defining $F_m(Q)$ as the following integral:

$$F_m(Q) = \int_{0}^{r} f_m v^*(Q,P) \rho d\rho, \tag{17}$$

we can write:

$$P(Q) = \sum_{m=1}^{M} \gamma_m \int_{\theta} F_m(Q) d\theta. \tag{18}$$

Considering an infinitesimal angle $d\theta$ (Figure 2), the relation between the arch length $rd\theta$ and the infinitesimal boundary length $d\Gamma$, can be written as:

$$\cos\alpha = \frac{r\frac{d\theta}{2}}{\frac{d\Gamma}{2}}, \tag{19}$$

or

$$d\theta = \frac{\cos\alpha}{r} d\Gamma, \tag{20}$$

where α is the angle between unity vectors $\mathbf{r}$ and $\mathbf{n}$.

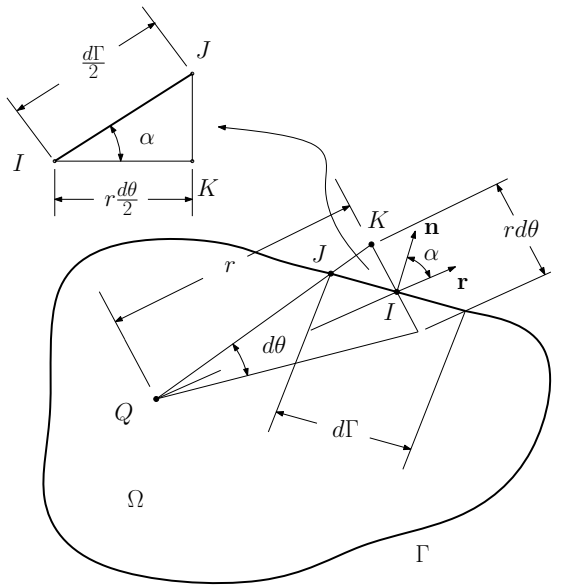

Figure 2: Geometric relation for the domain transformation.

Using the inner product properties of the unity vectors $\mathbf{n}$ and $\mathbf{r}$, showed in Figure 2, we can write:

$$d\theta = \frac{\mathbf{n}.\mathbf{r}}{r} d\Gamma. \tag{21}$$

Substituting equation (21) into equation (18), the domain integral (10) can be written as a boundary integral given by:

$$P(Q) = \sum_{m=1}^{M} \gamma_m \int_{\Gamma} \frac{F_m(Q)}{r} \mathbf{n}.\mathbf{r} d\Gamma, \tag{22}$$

or, in a matrix form:

$$P(Q) = \left[\begin{array}{cc} \int_{\Gamma} \frac{F_1(Q)}{r} \mathbf{n}.\mathbf{r} d\Gamma & \int_{\Gamma} \frac{F_2(Q)}{r} \mathbf{n}.\mathbf{r} d\Gamma \\ \multicolumn{2}{c}{\ldots \quad \int_{\Gamma} \frac{F_M(Q)}{r} \mathbf{n}.\mathbf{r} d\Gamma} \end{array} \right] \left\{ \begin{array}{c} \gamma_1 \\ \gamma_2 \\ \vdots \\ \gamma_M \end{array} \right\}. \tag{23}$$

To compute γ_m, it is necessary to consider the body force in M points of the domain and of the boundary. In the case of this work, these points are the boundary nodes and some internal points. Thus, equation (11) can be written as:

$$\mathbf{b} = \mathbf{F}\boldsymbol{\gamma}, \tag{24}$$

and γ can be computed as:

$$\gamma = \mathbf{F}^{-1}\mathbf{b}. \tag{25}$$

Substituting (25) into equation (23), we have:

$$P(Q) = \left[\begin{array}{cc} \int_\Gamma \frac{F_1(Q)}{r}\mathbf{n}.\mathbf{r}d\Gamma & \int_\Gamma \frac{F_2(Q)}{r}\mathbf{n}.\mathbf{r}d\Gamma \\ \ldots & \int_\Gamma \frac{F_M(Q)}{r}\mathbf{n}.\mathbf{r}d\Gamma \end{array} \right] \mathbf{F}^{-1}\mathbf{b}. \tag{26}$$

Writing equation (26) for all source points, i.e., all boundary nodes and internal points, we have the following matrix equation:

$$\mathbf{P} = \mathbf{R}\mathbf{F}^{-1}\mathbf{b} = \mathbf{S}\mathbf{b}, \tag{27}$$

where $\mathbf{S} = \mathbf{R}\mathbf{F}^{-1}$, $\mathbf{P}$ is a vector that contains the value of $P(Q)$ in all source points Q, and $\mathbf{R}$ is a matrix that contains the value of integrals of equation (26) when this equation is written for all source points Q.

4 Matrix equation

Considering all body forces that appears in equations (1), (3), and (4), the vector $\mathbf{P}$ for these equations are given by:

$$\mathbf{P} = \begin{bmatrix} \mathbf{0} & \mathbf{0} & \mathbf{S}^{mc}_{bb} & \mathbf{S}^{mc}_{bi} & \mathbf{S}^{mc}_{bc} \\ \mathbf{0} & \mathbf{0} & \mathbf{S}^{mc}_{ib} & \mathbf{S}^{mc}_{ii} & \mathbf{S}^{mc}_{ic} \\ \mathbf{S}^{p1c}_{bb} & \mathbf{S}^{p1c}_{bi} & \mathbf{S}^{p1}_{bb} & \mathbf{S}^{p1}_{bi} & \mathbf{S}^{p1}_{bc} \\ \mathbf{S}^{p2c}_{bb} & \mathbf{S}^{p2c}_{bi} & \mathbf{S}^{p2}_{bb} & \mathbf{S}^{p2}_{bi} & \mathbf{S}^{p2}_{bc} \\ \mathbf{S}^{p1c}_{ib} & \mathbf{S}^{p1c}_{ii} & \mathbf{S}^{p1}_{ib} & \mathbf{S}^{p2}_{ii} & \mathbf{S}^{p1}_{ic} \\ \mathbf{S}^{p1c}_{cb} & \mathbf{S}^{p1c}_{ci} & \mathbf{S}^{p1}_{cb} & \mathbf{S}^{p1}_{ci} & \mathbf{S}^{p1}_{cc} \end{bmatrix} \begin{Bmatrix} \mathbf{u}_b \\ \mathbf{u}_i \\ \mathbf{w}_b \\ \mathbf{w}_i \\ \mathbf{w}_c \end{Bmatrix} \tag{28}$$

where the superscript index of matrix $\mathbf{S}$ stands for the type of equation that is being used, i.e., m stands for the membrane equation given by equation (1), $p1$ stands for the first plate equation, given by equation (3), and $p2$ stands for the second plate equation, given by equation (4). The letter c in the superscript index means that these are coupling terms. In matrix $\mathbf{S}$, the first subscript index stands for the location of the source points (b if source points are at a smooth part of the boundary, i if they are in the domain and c if they are at corners). The second subscript index shows where are the body forces that are multiplied by terms of the matrix $\mathbf{S}$. For the second index, the same letters of the first subscript index are used with the same meaning. The right hand side vector has nodal values of the body forces that in this case are given by displacements (all the remaining terms of domain integrals are considered as part of the fundamental solution v^*). The letter $\mathbf{u}$ stands for displacements in the x_1 and x_2 directions and $\mathbf{w}$ stands for displacement in the transversal direction. Subscript indices in the right hand side vector indicate the location of nodes where displacements are computed.

Finally, if the boundary Γ is discretized in boundary elements and equations (1), (3), and (4) is written for all source points, the following matrix equation can be obtained:

$$\begin{bmatrix} \mathbf{H}^m_{bb} & \mathbf{0} & \mathbf{0} & \mathbf{0} & \mathbf{0} \\ \mathbf{H}^m_{ib} & \mathbf{I} & \mathbf{0} & \mathbf{0} & \mathbf{0} \\ \mathbf{H}^{p1c}_{bb} & \mathbf{0} & \mathbf{H}^{p1}_{bb} & \mathbf{0} & \mathbf{H}^{p1}_{bc} \\ \mathbf{H}^{p2c}_{bb} & \mathbf{0} & \mathbf{H}^{p2}_{bb} & \mathbf{0} & \mathbf{H}^{p2}_{bc} \\ \mathbf{H}^{p1c}_{ib} & \mathbf{0} & \mathbf{H}^{p1}_{ib} & \mathbf{I} & \mathbf{H}^{p1}_{ic} \\ \mathbf{H}^{p1c}_{cb} & \mathbf{0} & \mathbf{H}^{p1}_{cb} & \mathbf{0} & \mathbf{H}^{p1}_{cc} \end{bmatrix} \begin{Bmatrix} \mathbf{u}_b \\ \mathbf{u}_i \\ \mathbf{v}_b \\ \mathbf{w}_i \\ \mathbf{w}_c \end{Bmatrix}$$
$$= \begin{bmatrix} \mathbf{G}^m_{bb} & \mathbf{0} & \mathbf{0} \\ \mathbf{G}^m_{ib} & \mathbf{0} & \mathbf{0} \\ \mathbf{0} & \mathbf{G}^{p1}_{bb} & \mathbf{G}^{p1}_{bc} \\ \mathbf{0} & \mathbf{G}^{p2}_{bb} & \mathbf{G}^{p2}_{bc} \\ \mathbf{0} & \mathbf{G}^{p1}_{ib} & \mathbf{G}^{p1}_{ic} \\ \mathbf{0} & \mathbf{G}^{p1}_{cb} & \mathbf{G}^{p1}_{cc} \end{bmatrix} \begin{Bmatrix} \mathbf{t}_b \\ \mathbf{p}_b \\ \mathbf{p}_c \end{Bmatrix}$$
$$+ \begin{bmatrix} \mathbf{0} & \mathbf{0} & \mathbf{S}^{mc}_{bb} & \mathbf{S}^{mc}_{bi} & \mathbf{S}^{mc}_{bc} \\ \mathbf{0} & \mathbf{0} & \mathbf{S}^{mc}_{ib} & \mathbf{S}^{mc}_{ii} & \mathbf{S}^{mc}_{ic} \\ \mathbf{S}^{p1c}_{bb} & \mathbf{S}^{p1c}_{bi} & \mathbf{S}^{p1}_{bb} & \mathbf{S}^{p1}_{bi} & \mathbf{S}^{p1}_{bc} \\ \mathbf{S}^{p2c}_{bb} & \mathbf{S}^{p2c}_{bi} & \mathbf{S}^{p2}_{bb} & \mathbf{S}^{p2}_{bi} & \mathbf{S}^{p2}_{bc} \\ \mathbf{S}^{p1c}_{ib} & \mathbf{S}^{p1c}_{ii} & \mathbf{S}^{p1}_{ib} & \mathbf{S}^{p2}_{ii} & \mathbf{S}^{p1}_{ic} \\ \mathbf{S}^{p1c}_{cb} & \mathbf{S}^{p1c}_{ci} & \mathbf{S}^{p1}_{cb} & \mathbf{S}^{p1}_{ci} & \mathbf{S}^{p1}_{cc} \end{bmatrix} \begin{Bmatrix} \mathbf{u}_b \\ \mathbf{u}_i \\ \mathbf{w}_b \\ \mathbf{w}_i \\ \mathbf{w}_c \end{Bmatrix}$$
$$+ \mathbf{q} \tag{29}$$

where $\mathbf{H}$ and $\mathbf{G}$ are influence matrices of the BEM; the vector $\mathbf{v}$ contains transversal displacements and rotations of the nodes (not only transversal displacement as vector $\mathbf{w}$). Vectors $\mathbf{t}$ and $\mathbf{p}$ contain boundary node reactions for membrane and plate equations, respectively. The vector $\mathbf{q}$ is due to the domain load q_i. Domain integrals due to q_i's are transformed exactly into

boundary integrals using the procedure presented in Albuquerque, Sollero, Venturini, and Aliabadi (2006).

Equation (29) can be written in a more concise form as:

$$\mathbf{Hv} = \mathbf{Gt} + \mathbf{Su} + \mathbf{q} \tag{30}$$

Finally, columns of matrices of equation (30) can be reordered in accordance with boundary conditions and a linear equation system can be obtained where the unknown displacements and reactions can be computed.

5 Approximation functions

Two approximation functions are used in this work. The first is a radial basis function that has been used extensively in the DRM and is given by:

$$f_{m_1} = 1 + R. \tag{31}$$

The second is the well known thin plate spline:

$$f_{m_3} = R^2 \log(R), \tag{32}$$

used with the augmentation function given by equations (12) and (13). It has been shown in some works from literature that this approximation function can give excellent results for many different formulations [see Partridge (2000), and Golberg , Chen, and Bowman (1999)].

6 Characteristics of the radial integration method

An important advantage of the RIM over domain cell integration technique is that singularities that need to be treated in the cell integration are removed by the radial integration [Gao (2006)]. In this work, the domain integral of equation (1) is weak-singular because the derivatives of the fundamental solution $u^*_{ik,j}$ is of order $O(1/r)$. However, this singularity is removed due to the multiplication of derivatives of the fundamental solution by the radius ρ and also by the approximation function f_m in equation (17). So, regular numerical integration can be used in the computation of all domain integrals.

The most obvious advantage of the RIM over the DRM is that particular solutions do not need to be computed. Apart from that, the application of RIM to domain integrals like that given by equation (5) is straight forward while in the DRM it is necessary first to apply the Gauss theorem to eliminate the derivative of the fundamental solution. However, at the same time that the derivatives of the fundamental solution are eliminated, derivatives of transversal displacements appear in the DRM formulation. In order to avoid extra degrees of freedom in the DRM, Wen, Aliabadi, and Young (2000) proposed the approximation of derivatives of transversal the displacement by the nodal values of the transversal displacement multiplied by derivatives of the approximation function.

On the other hand, the most important disadvantage of the RIM is the computational cost to generate the matrix **S** that is considerably bigger than the DRM. In the RIM, the matrix **S** needs to be built by integration around the entirely boundary while in the DRM the integration is avoided by the use of the influence matrices **H** and **G**.

7 Numerical results

In order to compare its accuracy, the proposed method are applied to several numerical examples with various boundary conditions.

7.1 Circular spherical shallow shell

Consider a spherical shallow shell under pressure loading as shown in Figure 3. The geometry and material properties of the shell are as follows: thickness $h = 0.1$ m; radius of the base of the shell $a = 5$ m; curvature radii $R_1 = R_2 = R = 100$ m ($R_{12} = R_{21} = 0$), elastic modulus $E = 210$ GPa, and Poisson ratio $\nu = 0.3$. The internal pressure is $q_3 = q_o = 1$ MPa ($q_1 = q_2 = 0$). The edge of the shell is clamped, i.e., the boundary conditions are $u_1 = u_2 = w = \partial w/\partial n = 0$.

The transversal displacement is computed using approximation functions $1 + R$ and $R^2 \log(R)$. Two meshes are used: mesh 1 has 12 constant boundary elements and 9 internal points and mesh 2 has 24 constant boundary elements and 17 inter-

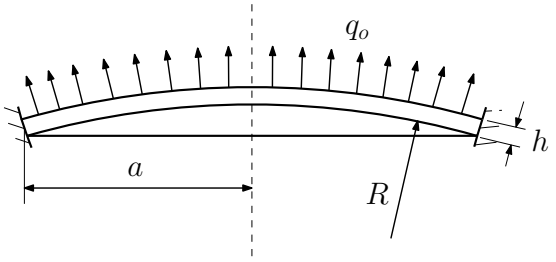

Figure 3: Clamped spherical shell under internal pressure.

nal points (mesh 2 is shown in Figure 4).

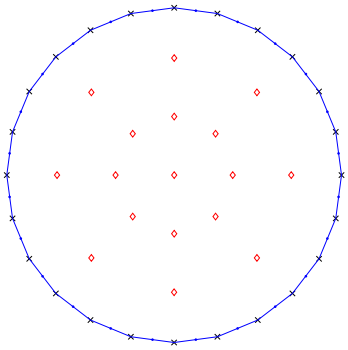

Figure 4: Mesh and internal points for the spherical shell (mesh 2, 24 boundary elements and 17 internal points).

Figure 5 shows transverse displacements of the shell computed using both approximation functions (approximation function 1 is $1+R$ and approximation function 2 is $R^2\log(R)$). Displacements are compared with results presented by Dirgantara and Aliabadi (1999) for the the same problem using a thick plate boundary element formulation. Other meshes with a higher number of nodes and internal points were used, however, as the results were almost coincident with the results presented by mesh 2, they will not be shown here. As it can be seen, the results of the proposed method converges to values slightly higher than those obtained by the thick plate formulation. It is also noted that both approximation functions presented quite similar results, especially with mesh 2 that has a higher number of nodes and internal points.

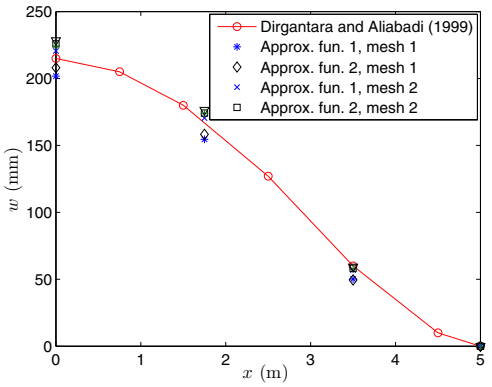

Figure 5: Transversal displacement for the spherical shell with clamped edge.

7.2 Circular spherical shallow shell with a hole in the centre

Consider now a circular spherical shallow shell with a hole in the centre as shown in Figure 6. The geometry and material properties of the shell are: radius of the base of the shell a = 5 m, radius of the hole b = 0.5 m, thickness h = 0.1 m, curvature radii $R_{11} = R_{22} = 200$ m ($R_{12} = R_{21} = 0$), elastic modulus $E = 210$ GPa, and Poisson ratio $\nu = 0.3$. The shell is under a uniformly distributed load $q_3 = q_o$ = 1 MPa, transversely applied ($q_1 = q_2 = 0$).

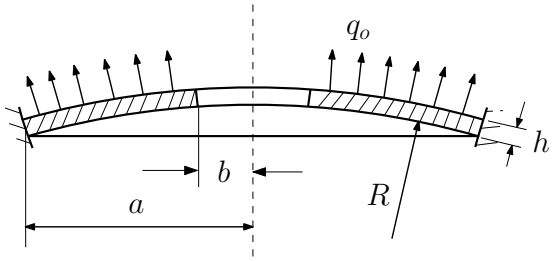

Figure 6: Circular spherical shallow shell with a hole in the centre under internal pressure.

This problem was analysed using two meshes: mesh 1 has 12 constant boundary elements in the outer boundary, 8 constant boundary elements in the inner boundary, and 10 internal points distributed uniformly in two rings (5 in each ring)

with radii equal to 3.5 m and 2.2 m and centre coincident with the center of the shell; mesh 2 has 24 constant boundary elements in the outer boundary, 16 constant elements in the inner boundary, and 20 internal points distributed uniformly in the two rings (10 in each ring). Mesh 2 is shown in Figure 7.

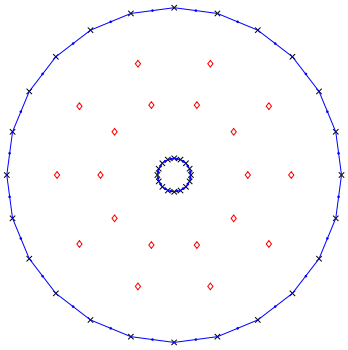

Figure 7: Boundary elements and internal points for the circular spherical shallow shell with a hole in the centre (mesh 2, 40 boundary elements and 20 internal points).

Figure 8 shows transverse displacements of the shell computed using the two approximation functions (again, approximation function 1 is $1+R$ and approximation function 2 is $R^2\log(R)$). Displacements are compared with results presented by Dirgantara (2002). As in the previous problem, it is also noted that both approximation functions presented quite similar results. This fact was unexpected because the use of the thin plate approximation function augmented by polynomials has significantly improved the accuracy in other applications of the RIM (see, for example Albuquerque, 2007). The results obtained with mesh 2 are in good agreement with Dirgantara (2000).

7.3 Square spherical shallow shell

In this example, a square spherical shallow shell, as shown in Figure 9, is analysed. The geometry and material properties of the shell are as follow: length of the base edge of the shell a =0.254 m, thickness h = 0.0127 m, curvature radii $R_1 = R_2 = R$ = 2.54 m ($R_{12} = R_{21} = 0$), elastic modulus

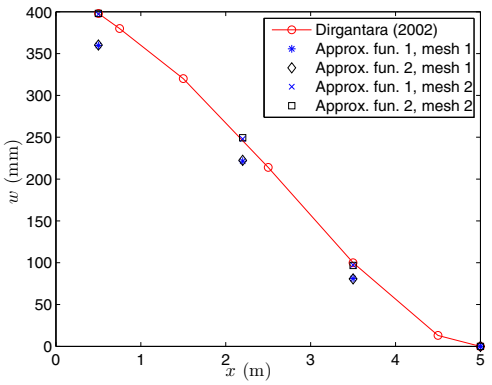

Figure 8: Transversal displacement for the circular spherical shallow shell with a hole in the centre.

E = 6.895 GPa, and Poisson ratio $\nu = 0.3$. The shell is under an uniformly distributed load in the transversal direction (internal pressure) q_3 = 2.07 MPa ($q_1 = q_2 = 0$).

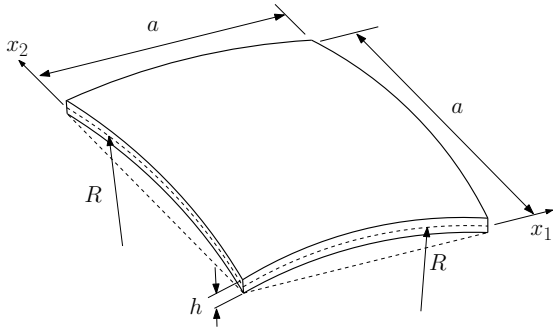

Figure 9: Square spherical shallow shell.

This problem was analysed considering two types of boundary conditions, i.e., clamped and simply-supported. Three meshes were used. Mesh 1 has 12 constant boundary elements and 9 internal points, mesh 2 has 20 boundary elements and 25 internal points, and mesh 3 has 28 boundary elements and 49 internal points. Mesh 3 is shown in Figure 10. All meshes have elements of equal length and uniformly distributed internal points. In this case, as in the previous, both approximation functions give quite similar results. Because this, only results obtained by approximation function 1, given by equation (31), will be shown for this example.

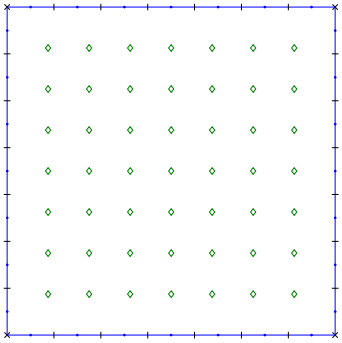

Figure 10: Boundary elements and internal points for the square spherical shallow shell (mesh 3, 28 boundary elements and 49 internal points).

Figures 11 and 12 show results for the clamped and simply-supported boundary conditions, respectively, together with meshless results obtained by Sladek, Sladek, Wen, and Aliabadi (2006) for the same problems.

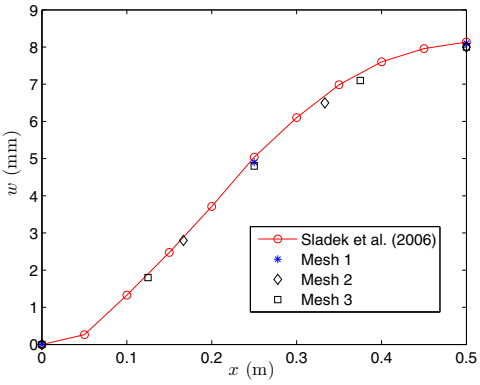

Figure 11: Transversal displacement for the square spherical shallow shell with clamped edges.

As it can be seen, the results for the clamped boundary conditions are in good agreement with the meshless results while for the simply-supported boundary conditions they are slightly lower. However, the convergence hasn't been achieved with these meshes. In order to show that there is convergence, this problem was analysed with a very refined mesh, with 124 elements (31 per edge) and 961 uniformly distributed internal points (31 $\times$ 31). Figure 13 shows results obtained with the very refined mesh.

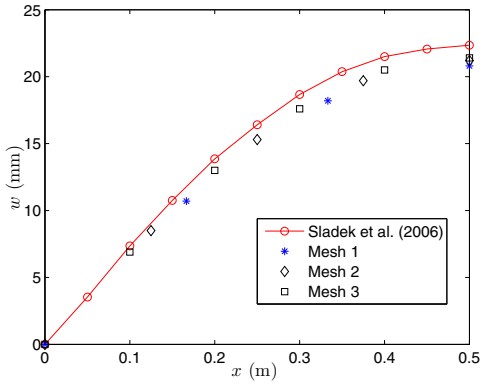

Figure 12: Transversal displacement for the square spherical shallow shell with simply-supported edges.

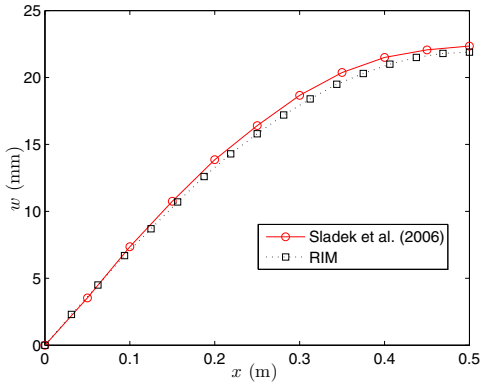

Figure 13: Transversal displacement for the square spherical shallow shell with simply-supported edges using a very refined mesh.

8 Conclusions

This paper presented a boundary element formulation for the analysis of thin shallow shells where domain integrals are transformed into boundary integrals by the radial integration method. As the radial integration method doesn't demand particular solutions, it is easier to implement than the dual reciprocity boundary element method. Besides, strong singularities in domain integrals are

cancelled by the radial integration. Two different approximation functions are used in the radial integration method. Results obtained with both approximation functions are in good agreement with results presented in literature. As in the dual reciprocity method, the accuracy of the method is improved by increasing the number of boundary nodes and internal points. However, different from dual reciprocity and even from other applications of the radial integration method, the use of radial basis function augmented by polynomials hasn't produced significantly changes in results.

Acknowledgement: The first author would like to thank the CNPq (The National Council for Scientific and Technological Development, Brazil) and AFOSR (Air Force Office of Scientific Research, USA) for financial support for this work.

References

Albuquerque, E. L.; Sollero, P.; W. P. Paiva. (2007): The radial integration method applied to dynamic problems of anisotropic plates. *Communications in Numerical Methods in Engineering*, vol. 23, pp. 805–818.

Albuquerque, E. L.; Sollero, P.; Venturini, W.; Aliabadi, M. H. (2006): Boundary element analysis of anisotropic Kirchhoff plates. *International Journal of Solids and Structures*, vol. 43, pp. 4029–4046.

Aliabadi, M. H. (2002): *Boundary element method, the application in solids and structures*. John Wiley and Sons Ltd, New York.

Baiz, P. M.; Aliabadi; M. H. (1999): Linear buckling of shear deformable shallow shells by the boundary domain element method. *CMES: Computer Modeling in Engineering & Sciences*, vol. 45, pp. 1257–1275.

Beskos, D. E. (1991): Static and dynamic analysis of shells. In D. E. Beskos, editor, *Boundary element analysis of plates and shells*, chapter 1, pages 93–140. Springer Verlag, Berlin.

Brebbia, C. A.; Debnath J. M. (1970): A comparison of recent shallow shell finite element analyses. *International Journal of Mechanical Sciences*, vol. 12, pp. 849–855.

Dirgantara, T. (2002): *A new boundary element formulation for shear deformable shells analysis*. WIT Press, Southampton.

Dirgantara, T.; Aliabadi, M. H. (1999): A new boundary element formulation for shear deformable shells analysis. *International Journal for Numerical Methods in Engineering*, vol. 45, pp. 1257–1275.

Gao, X. (2006): The radial integration method for evaluation of domain integrals with boundary only discretization. *Engineering Analysis with Boundary Elements*, vol. 13, pp. 19–34.

Gao, X. (2006): A meshless BEM for isotropic heat conduction problems with heat generation and spatially varying conductivity. *International Journal of Numerical Methods in Engineering*, vol. 66, pp. 1411–1431.

Golberg, M. A.; Chen, C. S.; Bowman, H. (1999): Some recent results and proposals for the use of radial basis functions in the BEM. *Engineering Analysis with Boundary Element*, vol. 23, pp. 285–296.

Lu, P.; Huang, M. (1992): Boundary element analysis of shallow shells involving shear deformation. *International Journal of Solids and Structures*, vol. 29, pp. 1273–1782.

Li, Q.; Soric, J.; Jarak, T.; Atluri, S. N. (2005): A locking-free meshless local Petrov-Galerkin formulation for thick and thin plates. *Journal of Computational Physics*, vol. 208, pp. 116–133.

Newton, D. A.; Tottenham, H. (1968): Boundary value problems in thin shallow shells of arbitrary plan form. *Journal of Engineering Mathematics*, vol. 2, pp. 211–223.

Partridge, P. W. (2000): Toward criteria for selection approximation functions in the dual reciprocity method. *Engineering Analysis with Boundary Elements*, vol. 24, pp. 519–529.

Partridge, P. W.; Brebbia, C. A.; Wrobel, L. C. (1992): *The dual reciprocity boundary element method*. Computational Mechanics Publications, Southampton, Boston.

Rabczuk, T.; Areias, P. (2006): A Meshfree thin shell for arbitrary evolving cracks based on an extrinsic basis. *CMES: Computer Modeling in Engineering and Sciences*, vol. 16, pp. 115–130.

Sladek, J.; Sladek, V.; Wen, P. H.; Aliabadi, M. H. (2006): Meshless local Petrov-Galerkin (MLPG) method for shear deformable shells analysis. *CMES - Computational Modelling in Engineering and Science*, vol. 13, pp. 103–117.

Wen, P. H.; Aliabadi, M. H.; Young, A. (2000): Application of dual reciprocity method to plates and shells. *Engineering Analysis with Boundary Elements*, vol. 24, pp. 583–590.

Zhang, J. D.; Atluri, S. N. (1986): A boundary/interior element method for quasi-static and transient response analysis of shallow shells. *Computers and Structures*, vol. 24, pp. 213–223.

Zhang, J. D.; Atluri; S. N. (1988): Post-buckling analysis of shallow shells by the field-boundary-element method. *International Journal for Numerical Methods in Engineering*, vol. 26, pp. 571–587.

Zhang, J. D.; O'Donoghue, P. E.; Atluri, S. N. (1986): Analysis of control of finite deformations of plates and shells, *Finite Element Methods for Plates and Shell Structures*, T. J. R. Hughes and E. Hinton, Eds., Chapter 6, Pineridge Press, Swansea, 127–153.